

Emergence of the 3D diluted Ising model universality class in a mixture of two magnets

J. J. Ruiz-Lorenzo,^{1,*} M. Dudka,^{2,3,4,†} M. Krasnytska,^{2,3,5,‡} and Yu. Holovatch^{2,3,6,7,§}

¹*Departamento de Física and Instituto de Computación Científica Avanzada (ICCAE),
Universidad de Extremadura, 06071 Badajoz, Spain*

²*Institute for Condensed Matter Physics, National Academy of Sciences of Ukraine, 79011 Lviv, Ukraine*

³^L⁴ *Collaboration & Doctoral College for the Statistical Physics of Complex Systems, Leipzig-Lorraine-Lviv-Coventry, Europe*

⁴*Lviv Polytechnic National University, 79013, Lviv, Ukraine*

⁵*Haiqu, Inc., Shevchenko St, 120G, Lviv, Ukraine, 79039*

⁶*Centre for Fluid and Complex Systems, Coventry University, Coventry, CV1 5FB, United Kingdom*

⁷*Complexity Science Hub Vienna, 1080 Vienna, Austria*

(Dated: November 25, 2024)

Usually, the impact of structural disorder on the magnetic phase transition in the 3D Ising model is analyzed within the framework of quenched dilution by a non-magnetic component, where some lattice sites are occupied by Ising spins, while others are non-magnetic. This kind of quenched dilution, according to the Harris criterion, leads to a change in the critical exponents that govern the asymptotics in the vicinity of the phase transition point. However, the inherent reason for the emergence of a new, random Ising model universality class is not the presence of a non-magnetic component but the disorder in structure of spin arrangement. To demonstrate this fact, in this paper, we set up extensive Monte Carlo simulations of a random mixture of two Ising-like magnets that differ in spin length s and concentration c . In doing so, we analyze the effect of structural disorder *per se* without appealing to the presence of a non-magnetic component. We support our numerical simulations with renormalization group calculations. Our results demonstrate the emergence of the 3D randomly diluted Ising model universality class in a random mixture of two Ising magnets. While the asymptotic critical exponents coincide with those known for the site-diluted 3D Ising model, the effective critical behavior is triggered by parameters s and c . The impact of their interplay is a subject of detailed analysis.

I. INTRODUCTION

The quenched structural disorder is inevitably present in real magnetic materials, inducing interesting features of their thermodynamic properties discriminating them from ideally structured counterparts. Therefore disordered magnets became widely used to analyze cooperative phenomena in systems with quenched disorder, for instance, in the vicinity of their phase transitions [1]. In particular, studies of the effects of disorder on critical behavior are of great importance not only from a fundamental point of view but also due to novel technological applications of structurally disordered materials [2].

The consequences of disorder depend on its nature [3]. In this paper, we address the case in which random structural imperfections are coupled to the local energy density (or, equivalently, a quenched local random transition temperature). The Harris criterion gives a qualitative answer about possible changes in the universality class under the influence of such weak quenched disorder [4]. It relates the change in the universality class of the structurally disordered system to the behavior of the heat capacity of its regular (pure) counterpart. If the

heat capacity of the regular system diverges, i.e. if the heat capacity critical exponent $\alpha_{\text{reg}} > 0$, then the structural disorder suppresses such divergency leading to the new asymptotics of the heat capacity with $\alpha_{\text{dis}} < 0$. It induces also the changes in other critical exponents, amplitude ratios and scaling functions, leading to the emergence of a new universality class. Since out of most common $O(m)$ -symmetrical magnets only the Ising magnets ($m = 1$) are characterized by the diverging heat capacity at space dimension $d = 3$, the main focus in the analysis of the emergence of the new universality class has been on the behavior of structurally-disordered quenched Ising magnets.

An archetypal example is given by diluted uniaxial magnetic alloys $\text{Fe}_x\text{Zn}_{1-x}\text{F}_2$, $\text{Mn}_x\text{Zn}_{1-x}\text{F}_2$ prepared by a substitution of a non-magnetic isomorph ZnF_2 for its antiferromagnetic counterpart (FeF_2 or MnF_2) [5–7]. Although it is known that “random magnets are substitutionally disorder materials in which several kinds of magnetic or non-magnetic ions are alloyed together” [1], still the most common examples of magnetic systems with local random transition temperature studied in experiments and Monte Carlo simulations are represented by diluted systems of magnetic and non-magnetic components. We refer to, for example, Refs. [8–11] for the numerical studies of these materials based on the 3D site-diluted Ising model.

From the theoretical perspective, the renormalization-group (RG) approach relates the emergence of the new

* ruiz@unex.es

† maxdudka@icmp.lviv.ua

‡ kras_mariana@icmp.lviv.ua

§ hol@icmp.lviv.ua

TABLE I. Universal exponents and cumulants for three-dimensional Ising models. As usual, ν is the correlation length exponent, η is the anomalous dimension of the field, ω is the correction-to-scaling exponent, $R_\xi = \xi/L$, U_4 is the Binder cumulant and g_2 is a cumulant measuring the lack of self-averageness of the systems (the last three cumulants computed at the critical point). First two rows: analytic estimates for the diluted Ising model universality class based on the resummed six-loop renormalization-group functions obtained within massive $d = 3$ approach (RG, 3D) [12] and minimal subtraction scheme (RG, MS) [13]. Number in *italic* gives η calculated from the scaling relation $\eta = 2 - \gamma/\nu$. The third and fourth rows: numerical Monte-Carlo (MC) simulations results for the exponents and cumulants of the 3D site-diluted Ising model. The fifth row: our MC results for the mixture of two Ising magnets differing in spin length, see Table V and Sec. III D for more details. In the four and fifth rows we provide the values of the first two leading correction-to-scaling exponents (hereafter, denoted as ω_1 and ω_2). The last row shows numerical estimates for the regular Ising model.

Model	ν	η	ω	R_ξ	U_4	g_2
RG, 3D [12]	0.675(19)	<i>0.024(79)</i>	0.15(10)	-	-	-
RG, MS [13]	0.678(10)	0.030(3)	0.25(10)	-	-	-
MC, Ising (site-diluted) [8]	0.6837(53)	0.037(4)	0.37(6)	0.598(4)	0.449(6)	0.145(3)
MC, Ising (site-diluted) [11]	0.683(2)	0.036(2)	0.33(3) and 0.82(8)			
Mixture of two Ising magnets, this paper	0.678(2)	0.033(7)	0.31(12) and 0.94(15)	0.5990(8)	0.453(3)	0.138(5)
MC, Ising [14, 15]	0.629912(86)	0.0362978(20)	0.8303(18)	0.6431(1)	0.46548(5)	0

universality class to the presence of the new random Ising fixed point of the RG transformation [16, 17]. Currently, the high-order RG series have been obtained and carefully analyzed to quantify critical behavior in the new universality class. Since very often the changes of critical properties of structurally disordered magnets are discussed in the context of presence of non-magnetic impurities, the new universality class is often named the 3D diluted Ising model universality class. Typical numerical values of the universal critical exponents and cumulants are given in Table I. They can be compared with the corresponding values of the regular 3D Ising model shown in the last row of the Table. I.

In our previous paper [18], considering the model for the random mixture of different magnetic compounds, we have shown that impurities are non necessary to be non-magnetic to cause the same effects on the critical behavior and the only key ingredient for its modifications is structural disorder itself. To this purpose, we appealed to the model of Ising-like spins of different lengths that was firstly introduced in the context of complex networks [19, 20] and adopted it for the regular lattice case. Using the replica method we have shown [18] that the Ising model with randomly distributed elementary spins of different lengths and the site-diluted Ising model (which contains magnetic and non-magnetic sites) are both described by the field-theoretical φ^4 effective Hamiltonians of the same symmetry, sharing therefore, the same universality class [12, 13, 16, 17, 21]. We have also analyzed the effective critical behavior of the mixture of two Ising magnets differing in spin length.

A confirmation of our findings was obtained for the two-dimensional Ising model with spins of two lengths [22] where critical exponents of pure two-dimensional Ising model were observed, that according to the Harris criterion [4] is expected also for the two-dimensional Ising random-site model.

The goal of this paper is to provide numerical support for the theoretically predicted scenario of the mere influ-

ence of structural disorder on the magnetic phase transition without resorting to dilution by the non-magnetic component. To this end, we set up intensive Monte Carlo simulations of the random binary mixture of Ising magnets with spin length ratio s and concentration c on a three-dimensional lattice. Our main result is summarized in the fifth row of Table I, where we give the values of the critical exponents and universal cumulants for the 3D mixture of the Ising magnet with smallest corrections to scaling ($s = 1.7$ and $c = 0.53$). To the best of our knowledge, this is the first numerical simulation that convincingly shows the emergence of the 3D diluted Ising universality class for the model with quenched disorder without resorting to the presence of non-magnetic components.

In addition, we will test, at a qualitatively level, the predictions of the perturbative RG on the behavior of the effective critical exponents confronting them with the results from numerical simulations.

The rest of this paper is organized as follows. In Sec. II, we introduce the model of a random mixture of two Ising-like magnets. Such a model enables one to analyze the effect of structural disorder *per se* without appealing to the presence of a non-magnetic component. We discuss some results for the asymptotic critical behavior of such a model and show that it belongs to the 3D diluted Ising model universality class. We also show that, depending on the particular choice of s and c , the critical behavior may be influenced by strong corrections to scaling, hence, the effective critical exponents may be observed. We describe our extensive Monte Carlo simulations in Sec. III. Our results demonstrate the emergence of the random Ising model universality class in a random mixture of two Ising magnets. While the asymptotic critical exponents coincide with those known for the 3D site-diluted Ising model, the effective critical behavior is triggered by parameters s and c . Finally, in Sec. IV, we present our results and discuss their implications. Supplementary calculations and discussions are provided

in Appendices A and B.

II. MODEL AND ANALYTICAL RESULTS

In this section we describe the model that will be used in Sec. III for numerical simulations. We also summarize some results from its renormalization group analysis [18] and suggest possible scenarios for the effective critical behavior.

A. Random spin length Ising model

In this paper we consider a lattice model describing a system of interacting classical elementary magnets, ‘spins’. A notorious distinction of this model from a classical Ising model is that although the spins keep Ising model symmetry (pointing only up and down) they can vary in length. The Hamiltonian of the random spin length Ising model in the absence of an external magnetic field reads [19]:

$$\mathcal{H} = -\frac{1}{2} \sum_{\mathbf{r} \neq \mathbf{r}'} J(|\mathbf{r} - \mathbf{r}'|) S_{\mathbf{r}} S_{\mathbf{r}'}, \quad S_{\mathbf{r}} = \pm \hat{L}_{\mathbf{r}}. \quad (1)$$

where the sum spans the sites of a D -dimensional hypercubic lattice, $J(r)$ is a short-range interaction and $\hat{L}_{\mathbf{r}}$ are i.i.d. quenched random variables governed by the distribution function

$$P(\{\hat{L}\}) = \prod_{\mathbf{r}} p(\hat{L}_{\mathbf{r}}). \quad (2)$$

Originally, the Hamiltonian (1) has been suggested in the context of collective behavior in complex systems [19, 20] and then it was further applied to analyze magnetic and spin-glass phase transition in random magnets [18, 22]. A system of interacting spins of a random length described by the Hamiltonian (1) is sketched in Fig.1 (a). Obviously, putting all $\hat{L}_{\mathbf{r}} = 1$ one arrives at usual 3D Ising model shown in Fig.1 (b). In our analysis we will be interested in the case shown in Fig.1 (c), when lattice sites are occupied by spins of two different lengths, a part of spins are of length $\hat{L}_{\mathbf{r}} = 1$, the others being of a fixed length $\hat{L}_{\mathbf{r}} = s$. When the concentration of spins of length 1 is c and the concentration of spins of length s is $1 - c$, the corresponding probability distribution is given by:

$$p(\hat{L}_{\mathbf{r}}) = c\delta(\hat{L}_{\mathbf{r}} - 1) + (1 - c)\delta(\hat{L}_{\mathbf{r}} - s). \quad (3)$$

It is straightforward to see that the widely studied diluted Ising model, in which part of the lattice sites are occupied by Ising spins and the other being non-magnetic (or empty), as shown in Fig. 1 (d) is included in the definition of $p(\hat{L}_{\mathbf{r}})$ by putting $s = 0$ in Eq. (3).

In the case of quenched structural disorder, when the spin of lengths $\hat{L}_{\mathbf{r}} = 1$ and $\hat{L}_{\mathbf{r}} = s$ are randomly distributed and fixed in a certain configuration $\{\hat{L}\}$, physical

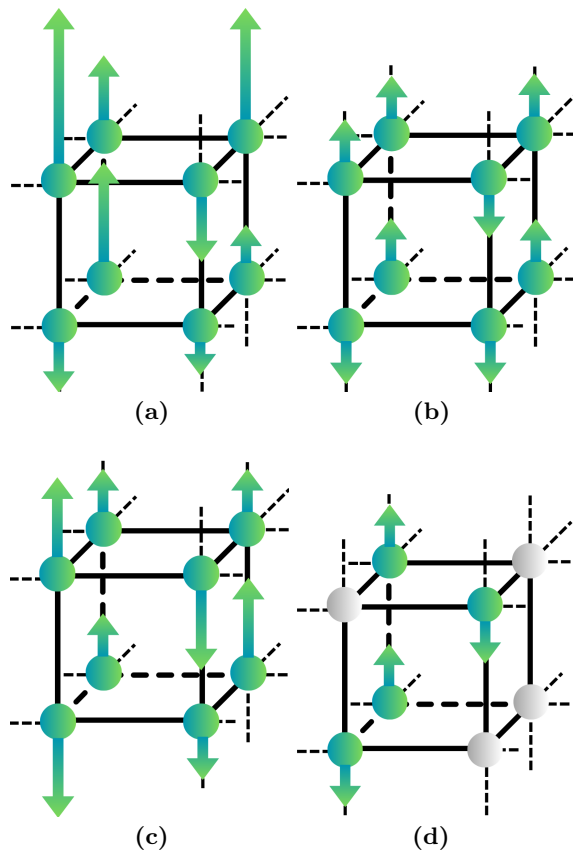


FIG. 1. Schematic representation of the (a) random spin length Ising model, when the lengths of spins are i.i.d. random variables, (b) standard 3D Ising model (with spins ± 1), (c) particular case of the random spin length Ising model: mixture of two Ising magnets with two different spin lengths (that will be analyzed henceforth), (d) diluted Ising model, where some sites (grey) are occupied by non-magnetic compounds or are empty.

observables are derived from the configurational average of the free energy [23]:

$$F = -\beta^{-1} \langle \ln Z(\{\hat{L}\}) \rangle_{\{\hat{L}\}}, \quad (4)$$

where $Z(\{\hat{L}\})$ is configuration-dependent partition function, the averaging over configurations is performed with the distribution function (3):

$$\langle \dots \rangle_{\{\hat{L}\}} = \prod_{\mathbf{r}} \sum_{\hat{L}_{\mathbf{r}}} p(\hat{L}_{\mathbf{r}}) (\dots). \quad (5)$$

The product in (5) is performed over all lattice sites and the sum over $\hat{L}_{\mathbf{r}}$ spans on the two values of $\hat{L}_{\mathbf{r}} = 1, s$.

In classical settings, one resorts on the replica approach [24] to perform the configurational averaging in (4). Representing the logarithm of the partition function in the form:

$$\ln Z(\{\hat{L}\}) = \lim_{n \rightarrow 0} \frac{(Z(\{\hat{L}\}))^n - 1}{n}, \quad (6)$$

and using Hamiltonian (1) one arrives at the following effective Hamiltonian [18] with two ϕ^4 terms of different symmetry

$$\mathcal{H}_{\text{eff}} = \frac{1}{2} \sum_{\mathbf{k}} \sum_{\alpha=1}^n \left(\frac{1}{\beta\nu(k)} - u_2 \langle \hat{L}^2 \rangle \right) \phi_{\mathbf{k}}^{\alpha} \phi_{-\mathbf{k}}^{\alpha} + \sum_{\mathbf{r}} \left(\frac{g_{1,0}}{4!} \sum_{\alpha,\beta=1}^n (\phi_{\mathbf{r}}^{\alpha})^2 (\phi_{\mathbf{r}}^{\beta})^2 + \frac{g_{2,0}}{4!} \sum_{\alpha=1}^n (\phi_{\mathbf{r}}^{\alpha})^4 \right) \quad (7)$$

where β is an inverse temperature, $\nu(k)$ is the Fourier transform of the interaction potential $J(r)$, and the coefficients of the different ϕ^4 terms can be expressed in terms of the moments of the random variable \hat{L} :

$$g_{1,0} = -3u_2^2 \left(\langle \hat{L}^4 \rangle - \langle \hat{L}^2 \rangle^2 \right),$$

$$g_{2,0} = u_4 \langle \hat{L}^4 \rangle,$$

with $u_2/2 = 1/2$, $u_4/4! = 1/12$. The moments of the random variable \hat{L} with the distribution function (3) readily follow:

$$\langle \hat{L}^k \rangle = c + (1-c)s^k, \quad (8)$$

$$\langle \hat{L}^4 \rangle - \langle \hat{L}^2 \rangle^2 = c(1-c)(1-s^2)^2. \quad (9)$$

With these expressions at hand, we get $g_{i,0}$ dependence on c and s via

$$g_{1,0} = -3c(1-c)(1-s^2)^2, \quad (10)$$

$$g_{2,0} = 2(c + (1-c)s^4). \quad (11)$$

There are two lessons to learn from the derivation of the effective Hamiltonian (7). The first, and an obvious one, is that its symmetry is the same as the one for the diluted Ising model, widely studied before by various approaches, see, e.g., Refs. [3, 16, 17] for reviews. This, in turn leads to the conclusion that the asymptotic critical behavior of the random mixture of two Ising magnets and that of the Ising magnet diluted by a non-magnetic isomorph coincide [18]. In particular, all renormalization group calculations performed so far to analyze asymptotic behavior of the diluted Ising model are directly applicable to our model too.

The second lesson can be obtained by observing, how the coefficients $g_{0,i}$, see Eqs. (10) and (11) depend on the concentration c and the difference in spin length s . Indeed, changing the values of c , s one can trigger the ratio

$$r(c, s) = \frac{g_{1,0}}{g_{2,0}} = -\frac{3c(1-c)(1-s^2)^2}{2(c + (1-c)s^4)}. \quad (12)$$

This ratio defines the starting conditions for the renormalization group flow that governs the approach of the couplings g_i to their fixed-point values upon renormalization. In Sec. II B we will study this effect in more detail to select appropriate parameter sets c and s and further exploit them in the numerical simulations presented in Sec. III.

B. Renormalization group flows and effective critical exponents

Being a powerful tool to calculate universal characteristics of critical behavior, the RG approach was successively used to treat critical behavior in a non-asymptotic regime, where the approach to criticality is characterized by non-universal effective critical exponents.

Among its achievements is the description of experimentally observed non-universal behavior of the amplitude ratio of thermal conductivity in ^4He , transport coefficients in ^3He - ^4He mixture, shear viscosity in Xe (see e.g. review [25]). It was also used to calculate effective critical exponents of diluted magnetic systems [26–29].

In our previous paper [18] we have studied effective critical behavior of the model, see Eqs. (1) and (3), analyzing the effective Hamiltonian (7) in the continuous limit by the field-theoretical RG methods [30–32]. In the following, we provide a brief explanation of the method and use it to select the model parameters that will use as input for the MC simulations in Sec. III.

In the continuous limit the effective Hamiltonian (7) can be rewritten using the notations of Ref. [13] as follows:

$$\mathcal{H}_{\text{eff}} = \int d^d \mathbf{r} \left\{ \frac{1}{2} \sum_{\alpha=1}^n [m_0^2 (\phi_{\mathbf{r}}^{\alpha})^2 + |\nabla \phi_{\mathbf{r}}^{\alpha}|^2] + \frac{g_{1,0}}{4!} \sum_{\alpha,\beta=1}^n (\phi_{\mathbf{r}}^{\alpha})^2 (\phi_{\mathbf{r}}^{\beta})^2 + \frac{g_{2,0}}{4!} \sum_{\alpha=1}^n (\phi_{\mathbf{r}}^{\alpha})^4 \right\} \quad (13)$$

where squared bare (unrenormalized) mass m_0^2 measures the distance in temperature τ to the critical point, and the ratio of bare couplings $g_{1,0}/g_{2,0}$ equals to $r(c, s)$, see Eq. (12).

Within the RG approach, a change in couplings g_1, g_2 (starting from the initial values given by Eqs. (10) and (11)) of the effective Hamiltonian (13) under the renormalization is described by the flow equations [30–32]:

$$\ell \frac{d}{d\ell} g_1(\ell) = \beta_{g_1}(g_1(\ell), g_2(\ell)), \quad \ell \frac{d}{d\ell} g_2(\ell) = \beta_{g_2}(g_1(\ell), g_2(\ell)), \quad (14)$$

where ℓ is the RG flow parameter.

The flow parameter can be related by means of a so-called ‘matching condition’ to the correlation length, depending on the temperature distance τ to the critical point, see e.g., Ref. [25]. In a simpler case, it is proportional to the inverse squared correlation length, therefore the limit $\tau \rightarrow 0$ corresponds to $\ell \rightarrow 0$. In this limit, $g_1(\ell)$ and $g_2(\ell)$ attain their stable fixed point (FP) values.

The FP (g_1^*, g_2^*) of the RG transformation is defined by means the zero of both β -functions: $\beta_{g_1}(g_1^*, g_2^*) = 0$, $\beta_{g_2}(g_1^*, g_2^*) = 0$. The FP is stable if both eigenvalues of the stability matrix

$$B_{ij} \equiv \frac{\partial \beta_{g_i}}{\partial g_j}, \quad i, j = 1, 2, \quad (15)$$

presents, in this FP, positive real parts.

If the stable FP is reachable from the initial conditions – recall that for the effective Hamiltonian (7) the initial conditions depend on c and s and lie in the region $g_1 \leq 0$, $g_2 > 0$, – it corresponds to the critical point of the system.

Furthermore, asymptotic values of the critical exponents are defined by the FP values of the RG γ -functions. In particular, the correlation length and pair correlation function (anomalous dimension of the field) exponents ν and η , respectively, are expressed in terms of the RG functions γ_ϕ and γ_{m^2} describing renormalization of the field ϕ and of the squared mass m^2 correspondingly [30–32]:

$$\nu^{-1} = 2 + \gamma_{m^2}(g_1^*, g_2^*), \quad \eta = 2\gamma_\phi(g_1^*, g_2^*). \quad (16)$$

In the RG scheme, the effective critical exponents are calculated in the region, where the couplings $(g_1(\ell), g_2(\ell))$ have not yet reached their FP values and depend on ℓ . In particular, for the exponents ν_{eff} and η_{eff} one gets [17]:

$$\begin{aligned} \nu_{\text{eff}}(\tau) &= \frac{1}{2 + \gamma_{m^2}\{g_1\{\ell(\tau)\}, g_2\{\ell(\tau)\}\}} + \dots, \\ \eta_{\text{eff}}(\tau) &= 2\gamma_\phi\{g_1\{\ell(\tau)\}, g_2\{\ell(\tau)\}\} + \dots, \end{aligned} \quad (17)$$

where the dots denote contribution proportional to the β -functions, coming from the change in the amplitude part of corresponding quantities. Usually, these parts can be neglected [25].

Since our model and the site-diluted Ising model share effective Hamiltonian (see Sec. II A) we can use the RG equations of the latter. In particular, in our calculations, we have used field-theoretical RG functions calculated in the minimal subtraction scheme of renormalization within the highest accessible six-loop approximation [13, 33]. They were obtained in the form of perturbative series in couplings and are known to be asymptotic at best.

Therefore, one needs to apply certain resummation techniques trying to restore their convergence and to extract reliable numerical estimates on their basis. The results discussed below are obtained on the basis of conformal Borel resummation [34] procedure generalized for a case of several couplings [12, 35, 36]. It is briefly described in the Appendix A, see also Ref. [18] for more details.

As it is well established by now, the RG flow equation for the effective Hamiltonian (13) is characterized by three FPs in the region $g_1 \leq 0$, $g_2 \geq 0$: Gaussian FP **G** ($g_1 = 0$, $g_2 = 0$), pure Ising model FP **I** ($g_1 = 0$, $g_2 \neq 0$) and random Ising model FP **R** ($g_1 \neq 0$, $g_2 \neq 0$). They are given in Fig. 2. Only FP **R** is stable. The values of the asymptotic critical exponents we have obtained at the FP **R**, used the outlined procedure, are: $\nu = 0.676$ and $\eta = 0.032$. As one can see from Table I, they are very close to the latest analytical estimates, see also the review in Ref. [13] for earlier data.

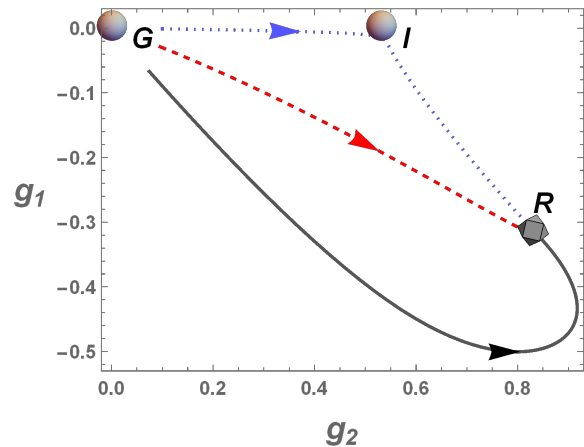


FIG. 2. Renormalization group flow in the space of couplings for different initial conditions. From up to down: $r = g_1(\ell_0)/g_2(\ell_0) = -0.01$ (dotted blue), -0.3 (dashed red), -0.9 (solid black). Unstable Gaussian (**G**) and Ising (**I**) FPs are shown by gray discs while a stable random Ising (**R**) FP is shown by the gray diamond.

Now let us proceed analyzing the RG picture in the non-asymptotic regime, to see how the effective critical exponents approach their asymptotic values depending on the initial couplings of the effective Hamiltonian.

Since we aim to verify analytic predictions by the MC simulation in the following section, let us present several effective exponents for selected initial conditions, which will serve as input for MC calculations afterwards.

To do that, we solve numerically the system of differential equations (14) with resummed β -functions getting the running values of the couplings. As already mentioned, the properties of the RG flow depend on the initial conditions $(g_1(\ell_0), g_2(\ell_0))$ of the differential equations (14). We have chosen $(g_1(\ell_0), g_2(\ell_0))$ in the vicinity of FP **G** for three distinct values $r = g_1(\ell_0)/g_2(\ell_0)$.

As one can see from the Fig. 2, all three flows lead to the stable FP with the decrease of ℓ . However, their behavior strongly depends on the initial conditions. For $r = -0.01$, the flow first stays within the basin of attraction of the unstable Ising FP (blue dotted curve in Fig. 2). For $r = -0.3$, the flow directly approaches the stable random FP (red dashed curve), while for $r = -0.9$, the running values of the couplings approach their stable FP values with ‘overshooting’ behavior (black curve).

The dependence of effective critical exponents ν_{eff} and η_{eff} on the flow parameter ℓ is presented in Fig. 3. Depending on the initial conditions, the effective critical exponent ν_{eff} either reaches its universal values at the stable FP comparatively fast (red curve), or attains the values that differ from the stable FP ones in a broad crossover region governed by the pure Ising model universality class critical exponents (blue curve), or its value exceeds the stable FP ones (peak in the black curve). We have not observed the third case for η_{eff} . A possible explanation is that the value of η is small, therefore the

approximation neglecting contributions marked by dots in Eq. (17) is not relevant to its calculation.

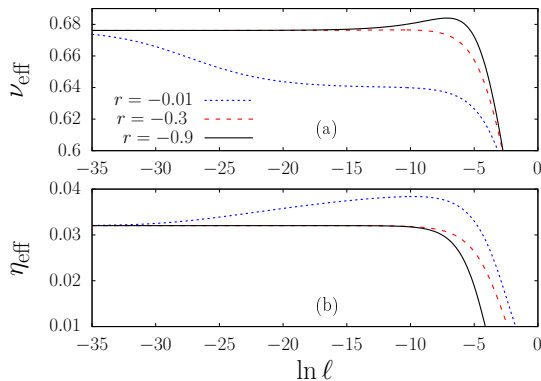


FIG. 3. Dependencies of the correlation length effective critical exponent ν_{eff} (top, panel (a)) and the pair correlation function effective critical exponent η_{eff} (bottom, panel (b)) on the flow parameter calculated along the RG flows of Fig. 2. Notice that we have used the same colors as in Fig. 2.

In the following section, we will check our theoretical predictions for the effective critical exponents for the flows with initial conditions $r = -0.3$ and $r = -0.9$. One can see from Eq.(12) that one option for the first case can be chosen as $s = 1.7$, $c \approx 0.53$, while for the second case, one can choose $s = 3$, $c \approx 0.79594$.

III. MONTE CARLO SIMULATIONS

In this section, we will describe the numerical methodology and the observables we have used in our analysis. After that, we will show our characterization of the critical properties of the model for two sets of model parameters.

A. The Model

Since we will consider the nearest neighbor interaction, it is convenient to re-write the Hamiltonian (1) as

$$\mathcal{H} = - \sum_{\langle r, r' \rangle} J_{r, r'} S_r S_{r'} \quad (18)$$

where the sum runs over all the nearest neighbors pairs in a three-dimensional cubic lattice of size L (and volume $V = L^3$) with periodic boundary conditions. The variables S_r are Ising ones (± 1). $J_{r, r'}$ are quenched variables (disorder) given by

$$J_{r, r'} = \hat{L}_r \hat{L}_{r'} \quad (19)$$

We recall that due to the distribution function (3) \hat{L}_r is 1 with probability c , otherwise s . Notice since all $J_{r, r'} > 0$ we can use cluster methods to simulate this model.

B. Observables

Let us introduce the magnetization per spin

$$\mathcal{M} = \frac{1}{V} \sum_r S_r. \quad (20)$$

Then the susceptibility can be written as

$$\chi = V \overline{\langle \mathcal{M}^2 \rangle}, \quad (21)$$

and the Binder cumulant as

$$U_4 = 1 - \frac{1}{3} \frac{\overline{\langle \mathcal{M}^4 \rangle}}{\overline{\langle \mathcal{M}^2 \rangle}^2}, \quad (22)$$

where $\langle (\dots) \rangle$ is the thermal average, $\overline{(\dots)}$ is the average over the disorder (length of the spins), and V is the number of lattice sites. In the thermodynamic limit $V \rightarrow \infty$, the Binder cumulant will be zero in the paramagnetic phase and will take the value $2/3$ in the ferromagnetic one.

A very useful way to characterize the phase transition is the use of the correlation length on a finite lattice [30, 37] defined as

$$\xi = \left(\frac{\chi/F - 1}{4 \sin^2(\pi/L)} \right)^{\frac{1}{2}}, \quad (23)$$

with

$$F = \frac{V}{3} \overline{\langle |\mathcal{F}(2\pi/L, 0, 0)|^2 + \text{two permutations} \rangle}, \quad (24)$$

\mathcal{F} being the Fourier transform of the magnetization

$$\mathcal{F}(\mathbf{k}) = \frac{1}{V} \sum_r e^{i\mathbf{k} \cdot \mathbf{r}} S_r. \quad (25)$$

Defined by Eq. (23), ξ is only a true correlation length in the paramagnetic phase, therefore, $R_\xi \equiv \xi/L$ goes to zero in this phase as L diverges. ξ will diverge in the ferromagnetic phase as $\xi \sim L^{d/2}$ and consequently R_ξ (in three dimensions). Therefore, the curves of R_ξ for different lattice sizes will cross near the critical temperature [30, 37].

To obtain the correlation length ν exponent from the analysis of R_ξ we need to estimate the derivative of the correlation length with respect to the inverse temperature $\beta = 1/T$, $\partial_\beta \xi$, by computing connected average values of different moments of the magnetization (and of \mathcal{F} in the case of ξ). The derivative for quantity $\overline{\langle \mathcal{O} \rangle}$ is calculated using the following relation

$$\partial_\beta \overline{\langle \mathcal{O} \rangle} = \overline{\partial_\beta \langle \mathcal{O} \rangle} = \overline{\langle \mathcal{O} \mathcal{H} - \langle \mathcal{O} \rangle \langle \mathcal{H} \rangle \rangle}. \quad (26)$$

To correct the bias induced by a small number of measurements in each sample we have applied a third-order extrapolation as described in Ref. [38].

The g_2 cumulant, measuring the lack of self-averageness of the system, is given by

$$g_2 = \frac{\overline{\langle \mathcal{M}^2 \rangle^2} - \overline{\langle \mathcal{M}^2 \rangle}^2}{\overline{\langle \mathcal{M}^2 \rangle}^2}. \quad (27)$$

The susceptibility will be a self-averaging quantity if g_2 tends to zero as L increases. If it is not the case, the susceptibility does not self-average (for example, see Refs. [39, 40]).

C. Simulation parameters

The model has been studied by means of numerical simulations. We have used a combination of the Wolff single-cluster algorithm [41] complemented by Monte Carlo local updates. In particular, our elementary Monte Carlo step (one sweep) consisted of L single-cluster updates, followed by a sequential full-lattice Metropolis update [8, 38, 42].

In addition, we have assessed the thermalization for each temperature monitoring against the logarithm of the Monte Carlo time non-local observables such as the susceptibility or the cumulant R_ξ . In Table II we report the parameters of our numerical simulations.

TABLE II. Parameters used in the numerical simulations. N_{samples} is the number of disorder realizations and N_{sweeps} is the number of the elementary Monte Carlo steps (built by L single-cluster updates, followed by a sequential full-lattice Metropolis update). Finally, the length of the spins is 1 with probability c and s with probability $1 - c$.

L	s	c	N_{samples}	N_{sweeps}	s	c	N_{samples}	N_{sweeps}
8	1.7	0.53	26000	256	3.0	0.795943	48440	256
12	1.7	0.53	26000	256	3.0	0.795943	48950	256
16	1.7	0.53	26000	256	3.0	0.795943	49000	256
24	1.7	0.53	36000	256	3.0	0.795943	49000	256
32	1.7	0.53	26070	256	3.0	0.795943	48996	256
48	1.7	0.53	28080	256	3.0	0.795943	48997	256
64	1.7	0.53	31440	256	3.0	0.795943	41725	256

In particular, we have simulated two sets of parameters: ($s = 1.7, c = 0.53$) for which the theory ($r = -0.3$) predicts small scaling corrections (almost a perfect action) and ($s = 3.0, c = 0.795943$) for which the prediction of the theory ($r = -0.9$) is the appearance of huge scaling corrections. Below, we will refer to the two simulated cases just as $s = 1.7$ and 3. Notice that we have computed the corresponding RG flows and effective exponents for these two values of r , see Fig. 3.

To simulate different temperatures we have performed an annealing from the highest temperature to the lowest one. For $s = 3$ we have simulated in the annealing procedure 20 temperatures in the critical region, for $s = 1.7$ we have simulated 20 temperatures for the smaller lattice sizes ($L \leq 32$) and 7 for $L = 48$ and 64. We have used a fifth-order polynomial-based analysis to compute the crossing temperatures.

D. Results

We have focused on the cumulant R_ξ to characterize the phase transition for both sets of parameters s and c . In Fig. 4 we show the curves $R_\xi(\beta)$ ($\beta = 1/T$) for the different lattice sizes and two values of s . The phase transitions are very clear for both values of s (the different curves cross at the apparent critical inverse temperature).

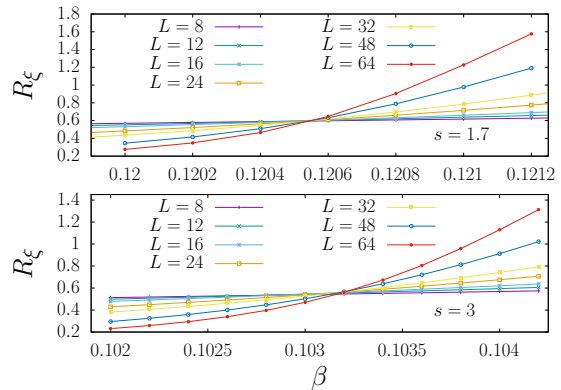


FIG. 4. Behavior of R_ξ versus the inverse temperature β for $s = 1.7$ (top) and $s = 3$ (below). The crossing point of the different curves marks the effective transition point.

We have analyzed these two phase transitions (for $s = 1.7$ and 3) using the quotients method [30, 43, 44], which is based on the analysis of the different observables on the crossing point of the curves L and $2L$, in this case of the cumulant R_ξ (we describe briefly this method in Appendix B). The intermediate data of this analysis based on the quotients method is reported in Table III (based on the crossing points of R_ξ) and IV (based on the crossing points of R_{g_2} and R_{U_4}).

One can take a much more detailed look at the data for the effective ν and η exponents by plotting them as a function of $1/L$ in order to check their asymptotic behavior, see Figs. 5 and 6, where we have also added the most accurate values from the 3D site-diluted Ising model [11]. Notice that the $s = 1.7$ -case is almost a perfect action (as predicted in Sec. II B by our RG analysis and for small values of L falls on the asymptotic value for both exponents). On the contrary, and again as predicted by our RG calculations, the $s = 3$ -case shows stronger scaling corrections.

A more quantitative analysis of the asymptotic values of the exponents ν and η and also the scaling correction exponents and the asymptotic values of the crossing points of R_ξ and U_4 (which are also universal) are presented in Table V. To obtain these asymptotic values, we have analyzed the effective ν and η exponents using Eq. (B3) and the values of R_ξ , g_2 and U_4 using Eq. (B4) (see Appendix B). In all the cases presented in this paper, the statistical qualities of the different fits are very good (the p -values of the χ^2 -fits are bigger than 0.05 in all the fits).

TABLE III. Quotients method results for the two simulated values of $s = 3$ and 1.7 from the crossing points of R_ξ for lattice sizes L_1 and L_2 .

s	L_1/L_2	β_{cross}	R_ξ	ν_ξ	η	Q_{U_4}
1.7	8/16	0.12051(1)	0.594(1)	0.694(2)	0.030(4)	0.984(1)
1.7	12/24	0.120552(6)	0.598(1)	0.684(2)	0.031(4)	0.991(1)
1.7	16/32	0.120550(4)	0.599(1)	0.680(2)	0.033(4)	0.992(1)
1.7	24/48	0.120549(2)	0.598(1)	0.679(2)	0.033(4)	0.995(1)
1.7	32/64	0.120555(1)	0.601(1)	0.678(2)	0.032(4)	0.995(1)
3.0	8/16	0.10289(1)	0.537(1)	0.757(3)	0.059(6)	0.982(2)
3.0	12/24	0.1031017)	0.550(1)	0.735(2)	0.044(5)	0.988(2)
3.0	16/32	0.103156(7)	0.556(1)	0.725(2)	0.039(5)	0.989(1)
3.0	24/48	0.103185(4)	0.561(1)	0.717(2)	0.036(5)	0.988(2)
3.0	32/64	0.103212(2)	0.567(1)	0.713(1)	0.034(6)	0.989(2)

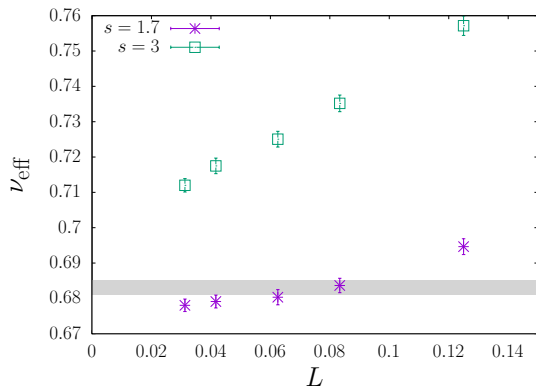


FIG. 5. Behavior of the effective exponent $\nu(L)$ computed with the quotients method as a function of $1/L$ for the two simulated cases $s = 1.7$ and 3.0. The shadow horizontal region is the most accurate value from numerical simulations [11] (one standard deviation).

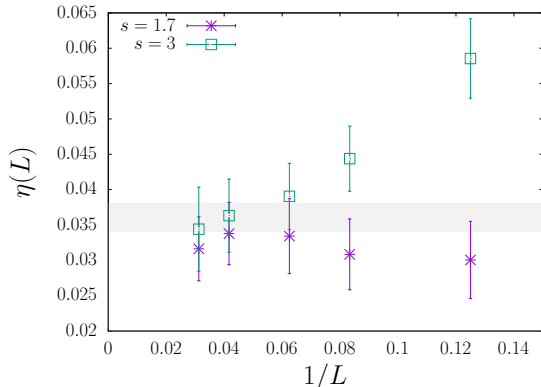


FIG. 6. Behavior of the effective exponent $\eta(L)$ computed with the quotients method as a function of $1/L$ for the two simulated cases $s = 1.7$ and 3.0. The shadow horizontal region is the most accurate value from numerical simulations [11] (one standard deviation).

η , g_2 , R_ξ and U_4 using a three-parameter fit, so, the ω exponent was not fixed finding that ω presented a large error. To compute the ω exponent we have analyzed the scaling of Q_{U_4} (see Eq. (B6)).

Notice that our final results for the universal quantities (see Table V) present a very good agreement (differences of less than 1.8 standard deviations in the worst case) with all the universal quantities of the 3D site-diluted Ising model, see Table I. It is important to notice that in the $s = 1.7$ -case we are obtaining a correction-to-scaling exponent that is very compatible with the sub-leading one of the 3D diluted Ising model ($\omega_2 = 0.82(8)$). However, in the $s = 3.0$ -case the computed omega exponent is compatible with the leading one ($\omega_1 = 0.37(6)$).

IV. CONCLUSIONS

In this paper, we have presented analytical and numerical analysis of the 3D Ising model in the presence of a disorder-inducing spin length variable providing a new view on how structural disorder affects magnetic phase transitions. We have computed the critical exponents and cumulants of this model for two values of the parameters finding a very good agreement with the critical exponents and cumulants of the 3D site-diluted Ising model as predicted by a perturbative field-theoretical RG analysis.

Furthermore, we have found that two simulated models, regarding their scaling corrections, behave as predicted by the field-theoretical RG analysis. We considered the limiting case for the model when spins can take two different lengths $\hat{L} = 1$ and $\hat{L} = s$. Based on RG analysis for effective exponents we simulated the critical behavior for the system with two sets of parameters: $s = 1.7$ (with concentration $c = 0.53$) and $s = 3$ (with concentration $c = 0.79594$). The RG analysis predicted different behavior for the scaling corrections. Using the quotients method, we observed distinct differences in scaling corrections for each case. Namely, for spin length $s = 1.7$ the obtained values align closely with the predicted asymptotic values for critical exponents, indicating minimal scaling corrections, whereas for $s = 3$

In particular, in Table V, we have extrapolated β_c , ν ,

TABLE IV. Quotients method results ($s = 3$ and 1.7) for the values of the cumulants g_2 and U_4 at the crossing points of R_{g_2} and R_{U_4} (respectively) for lattice sizes L_1 and L_2 .

s	L_1/L_2	U_4	g_2
1.7	8/16	0.4660(9)	0.113(1)
1.7	12/24	0.4616(9)	0.122(1)
1.7	16/32	0.4591(9)	0.127(1)
1.7	24/48	0.4559(7)	0.130(1)
1.7	32/64	0.4563(9)	0.134(2)
3.0	8/16	0.4525(9)	0.238(2)
3.0	12/24	0.456(1)	0.242(3)
3.0	16/32	0.457(1)	0.237(3)
3.0	24/48	0.457(1)	0.222(3)
3.0	32/64	0.459(1)	0.215(2)

TABLE V. Extrapolated results, using the quotients method, for $s = 1.7$ and $s = 3.0$.

s	ν	η	ω	R_ξ	U_4	g_2	β_c
1.7	0.678(2)	0.033(7)	0.94(15)	0.5990(8)	0.453(3)	0.138(5)	0.12056(1)
3.0	0.706(6)	0.033(7)	0.31(12)	0.579(8)	0.46(3)	0.13(1)	0.1033(1)

case the strong scaling corrections appear.

Therefore, we have confirmed our previous theoretical results obtained from the field-theoretical RG predictions [18] by MC simulations for the model with variable spin length. This leads to the strong conclusion that we can create new types of critical behavior in disordered Ising-like systems by considering systems with multiple magnetic components, where spin length and concentration can be used to fine-tune critical properties.

ACKNOWLEDGMENTS

M.D., M.K. and Yu.H were supported by the National Research Foundation of Ukraine Project 2023.03/0099 “Criticality of complex systems: fundamental aspects and applications”. J.J.R.L was partially supported by Ministerio de Ciencia, Innovación y Universidades (Spain), Agencia Estatal de Investigación (AEI, Spain, 10.13039/501100011033), and European Regional Development Fund (ERDF, A way of making Europe) through Grant No. PID2020-112936GB-I00, and by the Junta de Extremadura (Spain) and Fondo Europeo de Desarrollo Regional (FEDER, EU) through Grants No. GR21014 and No. IB20079. We have run our simulations in the computing facilities of the Instituto de Computación Científica Avanzada de Extremadura (ICCAEx).

Appendix A: Field-theoretical RG expansions and their resummation

In our calculations we have used the most up-to-date RG functions obtained for the effective Hamiltonian (13) with a record six-loop accuracy in the minimal subtraction renormalization scheme [13] (see also [33]). The

perturbative expansions for the RG functions are of the form:

$$\beta_{g_1}(g_1, g_2) = -g_1 \left(\varepsilon - \frac{8g_1}{3} - 2g_2 + \frac{14g_1^2}{3} + \frac{22g_1g_2}{3} + \frac{5g_2^2}{3} + \dots \right), \quad (\text{A1})$$

$$\beta_{g_2}(g_1, g_2) = -g_2 \left(\varepsilon - 4g_1 - 3g_2 + \frac{82g_1^2}{9} + \frac{46g_1g_2}{3} + \frac{17g_2^2}{3} + \dots \right), \quad (\text{A2})$$

$$\gamma_\phi(g_1, g_2) = \frac{g_1^2}{18} + \frac{g_1g_2}{6} + \frac{g_2^2}{12} + \dots \quad (\text{A3})$$

$$\gamma_{m^2}(g_1, g_2) = -g_2 - \frac{2g_1}{3} + \frac{5g_1^2}{9} + \frac{5g_1g_2}{3} + \frac{5g_2^2}{6} + \dots, \quad (\text{A4})$$

with $\varepsilon = 4 - d$ and the dots indicate higher order terms currently known up to $O(g_i^7)$ and $O(g_i^6)$ for the β - and γ -functions correspondingly [13, 33].

Usually, starting from the expressions for the RG functions, one can either develop the ε -expansion, or work directly at $d = 3$ considering the renormalized couplings (g_1, g_2) as the expansion parameters [45, 46]. However, such RG perturbation theory series are known to be asymptotic at best [31, 32]. Moreover, equations for FP are degenerated on a one-loop level in our particular case (see β -functions (A1) and (A2)). For this case, $\sqrt{\varepsilon}$ -expansion was elaborated [21, 47, 48], but it appears to have much worse convergent properties. Therefore we rely on the analysis of Eqs. (A1)–(A4) at fixed $d = 3$, putting there $\varepsilon = 1$ and analysing them as functions of couplings g_1 and g_2 .

One should apply appropriate resummation techniques

to improve the convergence of the RG perturbation series to get reliable estimates. Many different resummation procedures are currently used to this end, see e.g., Refs. [3, 16, 17]. In our study, we have used the method, based on the Borel transformation combined with a conformal mapping [34]. This resummation technique was first elaborated for field-theoretical models with one coupling. It requires knowledge about a high-order behavior of the series. This procedure was extended for field-theoretical models that contain several couplings [12, 35, 36]. For instance, it was used for the study of frustrated magnets modeled by field-theoretical effective Hamiltonian with two couplings [36, 49–51]. Although Borel summability has not been proven for perturbative series for models with disorder in $d > 0$ [35], the conformal Borel method has been successfully used for random Ising model [12, 25, 28, 52]. The following is a brief description of the procedure we use.

For the single variable case, the starting point is the infinite series

$$f(g) = \sum_{n=0}^{\infty} a_n g^n, \quad (\text{A5})$$

with the coefficients a_n growing factorially. Then, one defines Borel-Leroy transform by:

$$B(u) = \sum_{n=0}^{\infty} \frac{a_n}{\Gamma[n+b+1]} g^n, \quad (\text{A6})$$

where $\Gamma[\dots]$ is the Gamma-function. This transform is supposed to converge, in the complex plane, on the disk of radius $1/a$ where $g = -1/a$ is the singularity of $B(g)$ nearest to the origin. Then, using the integral representation of $\Gamma[n+b+1]$, $f(g)$ is rewritten as:

$$f(g) = \sum_{n=0}^{\infty} \frac{a_n}{\Gamma[n+b+1]} g^n \int_0^{\infty} dt e^{-t} t^{n+b}. \quad (\text{A7})$$

Then, interchanging summation and integration, one can define the Borel transform of f as:

$$f_B(u) = \int_0^{\infty} dt e^{-t} t^b B(gt). \quad (\text{A8})$$

In order to compute the integral in (A8) on the whole real positive semi-axis one needs an analytic continuation of $B(t)$. It may be achieved by several methods.

Notice that by using the conformal mapping technique, we assume that all the singularities of $B(u)$ lie on the negative real axis and that $B(u)$ is analytic in the whole complex plane excluding the cut from $-1/a$ to $-\infty$. Then, one can perform in B the change of variable $w(g) = \frac{\sqrt{1+ag}-1}{\sqrt{1+ag}+1} \iff g(w) = \frac{4}{a} \frac{w}{(1-w)^2}$. This change maps the complex g -plane cut from $g = -1/a$ to $-\infty$ onto the unit circle in the w -plane such that the singularities of $B(g)$ lying on the negative axis now lie on the boundary of the circle $|w| = 1$.

Finally, the resulting expression of $B(w(g))$ has to be re-expanded in powers of $w(g)$ and the resummed expression of the series f writes:

$$f_R(g) = \sum_{n=0}^{\infty} d_n(a, b) \int_0^{\infty} dt e^{-t} t^b [w(gt)]^n, \quad (\text{A9})$$

where $d_n(a, b)$ are the coefficients of the re-expansion of $B(g(w))$ in the powers of $w(g)$.

It is also useful to generalize the above expression (A9) in the following way [53]

$$f_R(g) = \sum_{n=0}^{\infty} d_n(\alpha, a, b) \int_0^{\infty} dt e^{-t} t^b \frac{[w(ut)]^n}{[1-w(ut)]^\alpha} \quad (\text{A10})$$

since this allows to impose the strong coupling behavior of the series: $f(g \rightarrow \infty) \sim g^{\alpha/2}$.

This procedure can be extended for field-theoretical models that contain several couplings. For instance, when f is a function of two variables g_1 and g_2 , the resummation technique can treat f as a function of coupling associated with terms related to the pure (e.g., not disordered) magnet (in our case it is g_2) and a ratio $z = g_1/g_2$, [12, 35, 36]:

$$f(g_2, z) = \sum_{n=0}^{\infty} a_n(z) g_2^n. \quad (\text{A11})$$

Then, keeping z fixed and performing the resummation only in g_2 according to the steps described above, one gets:

$$f_R(g_2, z) = \sum_{n=0}^{\infty} d_n(\alpha, a(z), b; z) \int_0^{\infty} dt e^{-t} t^b \frac{[w(g_2 t; z)]^n}{[1-w(g_2 t; z)]^\alpha}, \quad (\text{A12})$$

with z -dependent parameter $a(z)$. Here, as above, the coefficients $d_l(\alpha, a(z), b, z)$ in (A12) are computed so that the re-expansion of the right hand side of (A12) in powers of g_2 coincides with that of (A11).

Calculation of parameters a , b and α for the field-theoretical models with several couplings is a highly non-trivial task. Furthermore, in practice, procedure described above is applied to the truncated series (A1)-(A4), which are known up to the corresponding order of couplings. As a result, the resummed expansions (that usually correspond to certain physical observable) appear to be dependent on resummation parameters a , b and α . Often applying the conformal Borel method for models with two couplings, such parameters are taken in the region where physical observables are less sensitive to their values, see e.g., Ref. [49]. In our analysis we have tested the region of parameters discussed in the study of five-loop series for the model of frustrated magnet [49]: $a = 1/2$, b is varying in the interval [6, 30], while α is varying in $[-0.5, 2]$. As a final choice of the resummation parameters we get $a = 1/2$, $b = 10$ and $\alpha = 1$. At such values, the asymptotic critical exponents ν and η of the random Ising model are very close to the latest analytical estimates, see Table I.

Appendix B: Quotients method

In this appendix, we briefly describe the quotients method used to obtain extrapolated results for the critical exponents and scaling corrections presented in the paper.

Let $O(\beta, L)$ be a dimensionful quantity that scales in the thermodynamic limit as $\xi^{x_O/\nu}$. Notice that $x_O = 0$ for dimensionless observables. Furthermore, we will denote by the symbol g all the dimensionless quantities, like R_ξ , U_4 or g_2 .

The basis of the quotients method is to compare the same observable computed at L and $2L$

$$Q_O = \frac{O(\beta_{\text{cross}}(L, 2L), 2L)}{O(\beta_{\text{cross}}(L, 2L), L)}, \quad (\text{B1})$$

at $\beta_{\text{cross}}(L, 2L)$ which is defined by

$$g(L, \beta_{\text{cross}}(L, 2L)) = g(2L, \beta_{\text{cross}}(L, 2L)). \quad (\text{B2})$$

Therefore, one can write

$$Q_O^{\text{cross}} = 2^{x_O/\nu} + \mathcal{O}(L^{-\omega}), \quad (\text{B3})$$

and

$$g^{\text{cross}} = g^* + \mathcal{O}(L^{-\omega}), \quad (\text{B4})$$

where x_O/ν , g^* and the correction-to-scaling exponent ω are universal quantities. To compute the ν and η exponents, one should study dimensionful observables such as the susceptibility ($x_\chi = \nu(2 - \eta)$) and the β -derivatives of R_ξ and U_4 , both having $x = 1$.

The crossing point of the inverse temperature ($\beta_{\text{cross}}(L, 2L)$) scales as

$$\beta_{\text{cross}}(L, 2L) = \beta_c + A_{\beta_c, g} L^{-\omega-1/\nu} + \dots \quad (\text{B5})$$

Finally, the leading correction-to-scaling exponent can be estimated using the scaling of a dimensionless quantity g (Q_g) via

$$Q_g^{\text{cross}}(L) = 1 + A_g L^{-\omega} + B_g L^{-2\omega} + \dots \quad (\text{B6})$$

-
- [1] D. S. Fisher, G. M. Grinstein, and A. Khurana, Theory of Random Magnets, *Physics Today* **41**, 56 (1988).
- [2] Yu. Holovatch (editor), *See e.g., Order, Disorder and Criticality. Advanced Problems of Phase Transition Theory*, Vol. 1–7 (World Scientific, Singapore, 2004).
- [3] Y. Holovatch, V. Blavats'ka, M. Dudka, C. von Ferber, R. Folk, and T. Yavors'kii, Weak quenched disorder and criticality: resummation of asymptotic series, *International Journal of Modern Physics B* **16**, 4027 (2002).
- [4] A. B. Harris, Upper bounds for the transition temperatures of generalized Ising models, *Journal of Physics C: Solid State Physics* **7**, 3082 (1974).
- [5] R. J. Birgeneau, R. A. Cowley, G. Shirane, H. Yoshizawa, D. P. Belanger, A. R. King, and V. Jaccarino, Critical behavior of a site-diluted three-dimensional Ising magnet, *Phys. Rev. B* **27**, 6747 (1983).
- [6] D. P. Belanger, A. R. King, and V. Jaccarino, Crossover from random-exchange to random-field critical behavior in $\text{Fe}_x\text{Zn}_{1-x}\text{F}_2$, *Phys. Rev. B* **34**, 452 (1986).
- [7] P. W. Mitchell, R. A. Cowley, H. Yoshizawa, P. Böni, Y. J. Uemura, and R. J. Birgeneau, Critical behavior of the three-dimensional site-random Ising magnet: $\text{Mn}_x\text{Zn}_{1-x}\text{F}_2$, *Phys. Rev. B* **34**, 4719 (1986).
- [8] H. G. Ballesteros, L. A. Fernández, V. Martín-Mayor, A. Muñoz Sudupe, G. Parisi, and J. J. Ruiz-Lorenzo, Critical exponents of the three-dimensional diluted Ising model, *Phys. Rev. B* **58**, 2740 (1998).
- [9] P. Calabrese, V. Martín-Mayor, A. Pelissetto, and E. Vicari, Three-dimensional randomly dilute Ising model: Monte carlo results, *Phys. Rev. E* **68**, 036136 (2003).
- [10] D. Ivaneyko, J. Ihnytskyi, B. Berche, and Yu. Holovatch, Criticality of the random-site Ising model: Metropolis, swendsen-wang and wolff monte carlo algorithms, *Condens. Matt. Phys.* **8**, 149 (2005).
- [11] M. Hasenbusch, F. P. Toldin, A. Pelissetto, and E. Vicari, The universality class of 3d site-diluted and bond-diluted Ising systems, *Journal of Statistical Mechanics: Theory and Experiment* **2007**, P02016 (2007).
- [12] A. Pelissetto and E. Vicari, Randomly dilute spin models: A six-loop field-theoretic study, *Phys. Rev. B* **62**, 6393 (2000).
- [13] M. V. Kompaniets, A. Kudlis, and A. I. Sokolov, Critical behavior of the weakly disordered Ising model: Six-loop $\sqrt{\varepsilon}$ expansion study, *Phys. Rev. E* **103**, 022134 (2021).
- [14] A. M. Ferrenberg, J. Xu, and D. P. Landau, Pushing the limits of Monte Carlo simulations for the three-dimensional ising model, *Phys. Rev. E* **97**, 043301 (2018).
- [15] D. Simmons-Duffin, Bounds on 4D conformal and superconformal field theories, *High Energ. Phys.* **86**, [https://doi.org/10.1007/JHEP05\(2011\)017](https://doi.org/10.1007/JHEP05(2011)017) (2017).
- [16] A. Pelissetto and E. Vicari, Critical phenomena and renormalization-group theory, *Physics Reports* **368**, 549 (2002).
- [17] R. Folk, Y. Holovatch, and T. Yavors'kii, Critical exponents of a three-dimensional weakly diluted quenched Ising model, *Phys. Uspekhi* **46**, 169 (2003).
- [18] M. Dudka, M. Krasnytska, J. J. Ruiz-Lorenzo, and Y. Holovatch, Effective and asymptotic criticality of structurally disordered magnets, *JMMM* **575**, 170718 (2023).
- [19] M. Krasnytska, B. Berche, Y. Holovatch, and R. Kenna, Ising model with variable spin/agent strengths., *J. Phys. Complex* **1**, 035008 (2020).
- [20] M. Krasnytska, B. Berche, Y. Holovatch, and R. Kenna, Generalized ising model on a scale-free network: An interplay of power laws, *Entropy* **23**, 10.3390/e23091175 (2021).
- [21] G. Grinstein and A. Luther, Application of the renormal-

- ization group to phase transitions in disordered systems, *Phys. Rev. B* **13**, 1329 (1976).
- [22] G. Alfaro Miranda, L. F. Cugliandolo, and M. Tarzia, Swap algorithm for lattice spin models, *Phys. Rev. E* **110**, L043301 (2024).
- [23] R. Brout, Statistical mechanical theory of a random ferromagnetic system, *Phys. Rev.* **115**, 824 (1959).
- [24] V. Dotsenko, *Introduction to the Replica Theory of Disordered Statistical Systems* (Cambridge University Press, Cambridge, 2001).
- [25] R. Folk and G. Moser, Critical dynamics: a field-theoretical approach, *Journal of Physics A: Mathematical and General* **39**, R207 (2006).
- [26] H. K. Janssen, K. Oerding, and E. Sengespeick, On the crossover to universal criticality in dilute Ising systems, *Journal of Physics A: Mathematical and General* **28**, 6073 (1995).
- [27] R. Folk, Y. Holovatch, and T. Yavors'kii, Effective and asymptotic critical exponents of a weakly diluted quenched Ising model: Three-dimensional approach versus $\sqrt{\varepsilon}$ expansion, *Phys. Rev. B* **61**, 15114 (2000).
- [28] P. Calabrese, P. Parruccini, A. Pelissetto, and E. Vicari, Crossover behavior in three-dimensional dilute spin systems, *Phys. Rev. E* **69**, 036120 (2004).
- [29] M. Dudka, R. Folk, Y. Holovatch, and D. Ivaneiko, Effective critical behaviour of diluted Heisenberg-like magnets, *Journal of Magnetism and Magnetic Materials* **256**, 243 (2003).
- [30] D. J. Amit and V. Martin-Mayor, *Field Theory, The Renormalization Group and Critical Phenomena* (World Scientific, 2005).
- [31] J. Zinn-Justin, *Quantum Field Theory and Critical Phenomena* (Oxford University Press, 2002).
- [32] H. Kleinert and V. Schulte-Frohlinde, *Critical Properties of Φ^4 -Theories* (WORLD SCIENTIFIC, 2001) <https://www.worldscientific.com/doi/pdf/10.1142/4733>.
- [33] L. T. Adzhemyan, E. V. Ivanova, M. V. Kompaniets, A. Kudlis, and A. I. Sokolov, Six-loop ε expansion study of three-dimensional n -vector model with cubic anisotropy, *Nuclear Physics B* **940**, 332 (2019).
- [34] J. C. Le Guillou and J. Zinn-Justin, Critical exponents for the n -vector model in three dimensions from field theory, *Phys. Rev. Lett.* **39**, 95 (1977).
- [35] G. Álvarez, V. Martín-Mayor, and J. J. Ruiz-Lorenzo, Summability of the perturbative expansion for a zero-dimensional disordered spin model, *Journal of Physics A: Mathematical and General* **33**, 841 (2000).
- [36] P. Calabrese, P. Parruccini, A. Pelissetto, and E. Vicari, Critical behavior of $O(2) \otimes O(n)$ symmetric models, *Phys. Rev. B* **70**, 174439 (2004).
- [37] F. Cooper, B. Freedman, and D. Preston, Solving $\varphi_{1,2}^4$ field theory with Monte Carlo, *Nuclear Physics B* **210**, 210 (1982).
- [38] H. Ballesteros, L. Fernández, V. Martín-Mayor, A. Muñoz Sudupe, G. Parisi, and J. Ruiz-Lorenzo, The four-dimensional site-diluted Ising model: A finite-size scaling study, *Nuclear Physics B* **512**, 681 (1998).
- [39] S. Wiseman and E. Domany, Lack of self-averaging in critical disordered systems, *Phys. Rev. E* **52**, 3469 (1995).
- [40] A. Aharony and A. B. Harris, Absence of self-averaging and universal fluctuations in random systems near critical points, *Phys. Rev. Lett.* **77**, 3700 (1996).
- [41] U. Wolff, Collective Monte Carlo updating for spin systems, *Phys. Rev. Lett.* **62**, 361 (1989).
- [42] H. G. Ballesteros, L. A. Fernández, V. Martín-Mayor, A. Muñoz Sudupe, G. Parisi, and J. J. Ruiz-Lorenzo, Critical exponents of the three-dimensional diluted Ising model, *Phys. Rev. B* **58**, 2740 (1998).
- [43] M. Nightingale, Scaling theory and finite systems, *Physica A: Statistical Mechanics and its Applications* **83**, 561 (1976).
- [44] H. G. Ballesteros, L. A. Fernandez, V. Martín-Mayor, and A. Muñoz Sudupe, New universality class in three dimensions?: the antiferromagnetic RP^2 model, *Phys. Lett. B* **378**, 207 (1996), [arXiv:hep-lat/9511003](https://arxiv.org/abs/hep-lat/9511003).
- [45] R. Schloms and V. Dohm, Renormalization-group functions and nonuniversal critical behaviour, *Europhysics Letters* **3**, 413 (1987).
- [46] R. Schloms and V. Dohm, Minimal renormalization without ε -expansion: Critical behavior in three dimensions, *Nuclear Physics B* **328**, 639 (1989).
- [47] D. E. Khmel'nitskii, Second-order phase transition in inhomogeneous bodies, *Sov. Phys. JETP* **41**, 981 (1975).
- [48] T. C. Lubensky, Critical properties of random-spin models from the ε expansion, *Phys. Rev. B* **11**, 3573 (1975).
- [49] B. Delamotte, Y. Holovatch, D. Ivaneyko, D. Mouhanna, and M. Tissier, Fixed points in frustrated magnets revisited, *Journal of Statistical Mechanics: Theory and Experiment* **2008**, P03014 (2008).
- [50] B. Delamotte, M. Dudka, Y. Holovatch, and D. Mouhanna, Relevance of the fixed dimension perturbative approach to frustrated magnets in two and three dimensions, *Phys. Rev. B* **82**, 104432 (2010).
- [51] B. Delamotte, M. Dudka, Y. Holovatch, and D. Mouhanna, Analysis of the 3d massive renormalization group perturbative expansions: a delicate case, *Condensed Matter Physics* **13**, 43703 (2010).
- [52] A. S. Krinitsyn, V. V. Prudnikov, and P. V. Prudnikov, Calculations of the dynamical critical exponent using the asymptotic series summation method, *Theoretical and Mathematical Physics* **147**, 561–575 (2006).
- [53] D. I. Kazakov, O. V. Tarasov, and D. V. Shirkov, Analytic continuation of the results of perturbation theory for the model $g\phi^4$ to the region $g \gtrsim 1$, *Theoretical and Mathematical Physics* **38**, 9–16 (1979).